Stereoselectivity in the Salt–Cocrystal Products formed by Phenylglycinol or Phenylglycine with their Respective Sodium or Hydrochloride Salts

HARRY G. BRITTAIN
Center for Pharmaceutical Physics, Milford, New Jersey

ABSTRACT The salt and stereoselective cocrystal phenomena associated with 2-phenylglycinol and 2-phenylglycine have been studied using X-ray powder diffraction and differential scanning calorimetry. The chiral identities of the free acids and their sodium salts, or the free bases and their chloride salts, were found to play a determining role as to whether a salt–cocrystal product could or could not be formed. In particular, when cocrystallization of an enantiomerically pure basic or zwitterionic substance with its enantiomerically pure acid addition salt was attempted, a salt–cocrystal was only obtained when the absolute configuration of the two reactants is opposite. On the other hand, it has been found that no stereoselectivity in salt–cocrystal formation existed in the cocrystallization of an enantiomerically pure acidic or zwitterionic substance with its enantiomerically pure base addition salt. *Chirality 00:000-000, 2012.*

KEY WORDS: cocrystal; stereoselectivity; X-ray diffraction; thermal analysis,phenylglycinol; phenylglycine

INTRODUCTION

One of the impediments encountered in pharmaceutics today is that many drug substances exhibit less-than-desirable degrees of aqueous solubility. Various formulation and drug substance modification approaches have been brought to bear on this issue, and one of the more intriguing advances has been through the emergence of pharmaceutical cocrystals [1–3] and the effects that cocrystallization can have on water solubility. [4–6] Aakeröy has proposed that a cocrystal is a homogeneous crystalline solid that contains stoichiometric amounts of discrete neutral molecular species that are solids under ambient conditions, [7] and Schultheiss and Newman have summarized six definitions of a cocrystal that go further. [8]

Since the coformers making up both salt and cocrystal systems contain acidic donor and basic acceptor functionalities, it is clear that the ionization state and degree of proton transfer in an isolated product is essential to knowing whether one has prepared a cocrystal or a salt. [9–11] This situation was amply demonstrated in the cocrystallization of minoxidil with a variety of carboxylic acids, where seven salts and only one cocrystal product were actually isolated. [12]

The salt-or-cocrystal distinction is ordinarily made on the basis of atomic positions in a single-crystal structural determination, but this approach presents difficulties when a crystal of suitable quality cannot be obtained. Recognizing that the vibrational frequencies of bonded atoms involved in salt and cocrystal interactions would be perturbed to a lesser or greater degree depending on the nature of the proton transfer, studies have been carried out on cocrystals formed by salts of benzenecarboxylic acids with their respective free acids with the aim of developing selection rules for the recognition of cocrystal behavior. [13,14]

Recently, the first example of cocrystal solid solutions for a system containing enantiomers of opposite chirality has been reported for the 1:2 product formed by 4,4′-dipyridyl and ibuprofen. [15] In this work, it was found that the cocrystal products exhibited significantly higher melting temperatures and enthalpies of fusion relative to their parent ibuprofen chiral crystals, and the solid solutions could be crystallized to obtain a chiral enrichment. More recently, stereoselectivity in the salt–cocrystal products of α-methylbenzylamine and α-methyl-benzylammonium chloride was demonstrated, where formation of a salt–cocrystal product could take place only if the enantiomeric identities of the salt and free base were of opposite absolute configuration. [16]

The methylbenzylamine salt–cocrystal study just mentioned is of particular importance, as many compounds of pharmaceutical interest are basic in nature and very frequently are formulated in the form of their chloride salts. [17] With the recognition that exploitation of anion coordination and anion-templated assembly can yield new and interesting structures, [18] there has arisen a driving force to improve the physical properties of drug substances through cocrystal formation. Thus, salt–cocrystals of fluoxetine hydrochloride were prepared with benzoic, succinic, and fumaric acids, and the resulting perturbation on dissolution and solubility behavior evaluated. [19] Similarly, the physical properties of the salt–cocrystal of tiotropium fumarate with fumaric acid have been studied, and the product was reported to be the most stable solid form of the drug substance under ambient conditions. [20]

To investigate these phenomena in more detail, and to determine the generality of the observed stereoselectivity reported for the α-methylbenzylamine/α-methylbenzylammonium chloride salt–cocrystal system, [16] the products formed by the enantiomers of 2-phenylglycinol and 2-phenylglycine with their corresponding hydrochloride or sodium salts have been investigated. As evident in Figure 1, the cocrystal formers of the previous and present study can be viewed as being systematically substituted derivatives of benzylamine. The

*Correspondence to: Harry G. Brittain, Center for Pharmaceutical Physics, 10 Charles Road, Milford, New Jersey 08848. E-mail: hbrittain@centerpharmphysics.com
Received for publication 29 December 2011; Accepted 02 July 2012
DOI: 10.1002/chir.22103
Published online in Wiley Online Library (wileyonlinelibrary.com).

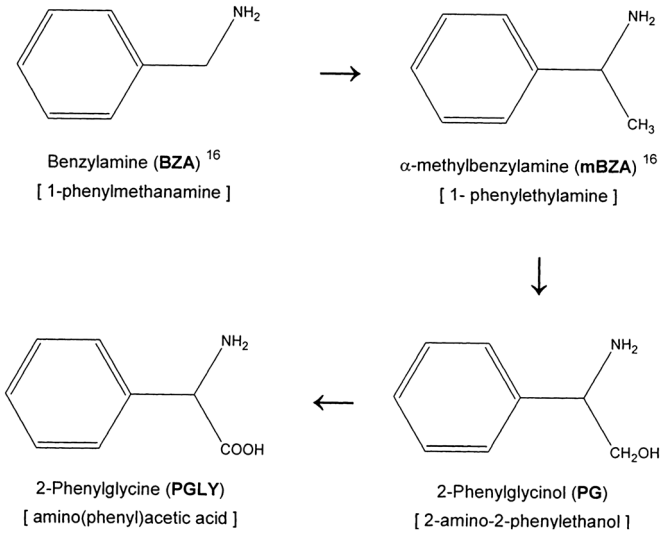

Fig. 1. Hierarchy in the structures of the chiral cocrystal formers, with reference to the preceding article.

formation of a particular salt–cocrystal product (or the absence of its formation) was demonstrated by means of X-ray powder diffraction, differential scanning calorimetry, and the total volatile content (TVC).

MATERIALS AND METHODS

General Procedures

X-ray powder diffraction (XRPD). XRPD patterns were obtained using a Rigaku (Woodlands, Texas, USA) MiniFlex powder diffraction system (X-ray source being nickel-filtered Kα emission of copper), equipped with a horizontal goniometer operating in the /2 mode. Samples were packed into the sample holder using a back-fill procedure and were scanned over the range of 3.5 to 40 degrees 2 at a scan rate of 0.5 degrees 2/min. Using a data acquisition rate of 1 point per second, these scanning parameters equate to a step size of 0.0084 degrees 2. XRPD patterns were indexed using the Rigaku PDXL software package, which enables pattern analysis by means of DICVOL,[21] ITO,[22] or N-TREOR.[23]

Differential scanning calorimetry (DSC). DSC thermograms were obtained on a TA Instruments (New Castle, Delaware, USA) 2910 thermal analysis system. Samples of approximately 1–2 mg were accurately weighed into an aluminum DSC pan, and then covered with an aluminum lid that was crimped in place. Samples were heated at a rate of 10 °C/min from ambient temperature to termination temperatures in the range of 150 to 225 °C, depending on the system under study.

TVC. Measurements of total volatile were made using an Ohaus (Parsippany, New Jersey, USA) model MB45 system. The samples were heated isothermally at a temperature of 110 °C for a period of 15 min, and the percentage of lost weight recorded. In some cases, it was noted that the samples had melted without significant weight loss.

Synthesis Procedures

Starting materials. (*R*)- and (*S*)-2-phenylglycinol and (*R*)- and (*S*)-2-phenylglycine were obtained from Aldrich (Milwaukee, Wisconsin, USA). Prior to their characterization, samples were wetted with methanol and ground to dryness in a mortar.

Salt preparation. The sodium salts of the 2-phenylglycine enantiomers were prepared by dissolving approximately 250 mg quantities in 10 ml of methanol, to which was added a 1:1 stoichiometric amount of 1.0*N* sodium hydroxide solution. The solutions were allowed to evaporate to dryness, whereupon the recovered solids were transferred to a mortar, wetted with methanol, and ground until a dry solid was obtained. The chloride salts of the 2-phenylglycinol and 2-phenylglycine enantiomers were prepared in a similar manner, namely, by dissolving approximately 250 mg quantities in 10 ml of methanol, added a 1:1 stoichiometric amount of 1.0*N* hydrochloric acid, evaporating to dryness, transferring the solids to a mortar, wetting with methanol, and grinding to dryness.

Salt–cocrystal preparation. Cocrystal products were prepared using the wet-grinding method,[24] where accurately weighed, equimolar amounts of free amine and the corresponding chloride salt (or free acid and the corresponding sodium salt) were placed in a mortar, wetted with methanol, and then ground to dryness.

RESULTS AND DISCUSSION

The 2-Phenylglycinol System

Since the XRPD patterns of (*S*)- and (*R*)-2-phenylglycinol (i.e., *S*-PG and *R*-PG, respectively) must necessarily be the same, as would the XRPD patterns of (*S*)- and (*R*)-2-phenylglycinol hydrochloride(i.e., *S*-PG-Cl and *R*-PG-Cl, respectively), only the patterns of the(*S*)-enantiomers have been shown in Figure 2. This figure also contains the XRPD patterns of the product isolated after the solvent-drop grinding of *S*-PG with *S*-PG-Cl, as well as the product resulting from the solvent-drop grinding of *S*-PG with *R*-PG-Cl. Detailed examination of the diffraction patterns indicated that the XRPD of the (*S*-PG) + (*S*-PG-Cl) product is simply the merged sum of the XRPD patterns of *S*-PG and *S*-PG-HCl, while the XRPD pattern obtained for the (*S*-PG)–(*R*-PG-HCl) product is definitely different from the XRPD patterns of its coformers. These observations are interpreted to indicate that the interaction of *S*-PG with *R*-PG-Cl yields an authentic salt–cocrystal, while the attempted interaction of *S*-PG with *S*-PG-Cl does not.

To further establish the authenticity of the (*S*-PG)–(*R*-PG-Cl) salt–cocrystal product, and the inability to cocrystallize *S*-PG and *S*-PG-Cl, an indexing analysis of the four XRPD patterns of Figure 2 was carried out. It was found that the XRPD patterns of *S*-PG, *S*-PG-Cl, and the (*S*-PG)–(*R*-PG-Cl) salt–cocrystal could be indexed so that a single set of unit cell parameters (which have been collected in Table 1) enabled a calculation of all major peaks in the respective diffraction patterns. Also included in Table 1 are the scattering angles and relative intensities of

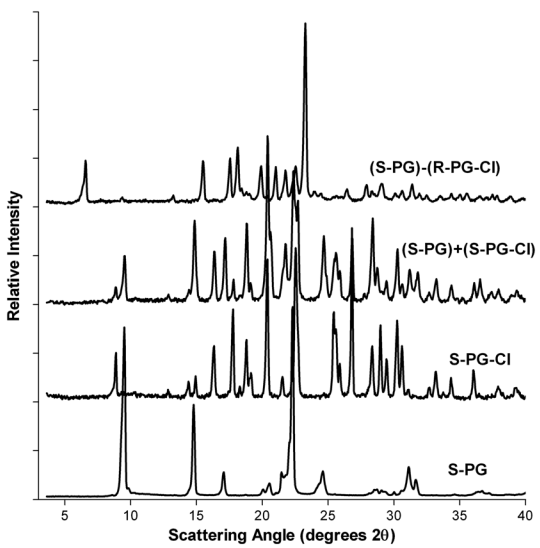

Fig. 2. X-ray powder diffraction patterns of (*S*)-phenylglycinol, (*S*)-phenylglycinol hydrochloride, the isolated yield of 1:1 (*S*)-phenylglycinol and (*S*)-phenylglycinol hydrochloride, and the 1:1 salt–cocrystal of (*S*)-phenylglycinol and (*R*)-phenyl-glycinol hydrochloride.

TABLE 1. Unit cell parameters obtained through indexing the X-ray diffraction patterns of (*S*)-phenylglycinol, (*S*)-phenylglycinol hydrochloride, and their 1:1 salt–cocrystal product, and the indexed listing of scattering peaks

Unit cell parameter	(*S*)-Phenylglycinol			(*S*)-Phenylglycinol hydrochloride			(*S*)-Phenylglycinol/(*R*)-phenylglycinol hydrochloride salt–cocrystal		
System	Monoclinic			Orthorhombic			Monoclinic		
a	18.471 Å			19.832 Å			5.870 Å		
b	9.248 Å			7.226 Å			26.749 Å		
c	8.635 Å			6.448 Å			5.457 Å		
α	90°			90°			90°		
β	90.94°			90°			93.70°		
γ	90°			90°			90°		
	Miller index	Angle (degree 2)	Relative intensity	Miller index	Angle (degree 2)	Relative intensity	Miller index	Angle (degree 2)	Relative intensity
	(0 1 0)	9.51	88.4	(2 0 0)	8.89	28.1	(0 2 0)	6.59	24.1
	(1 1 1)	14.79	48.7	(1 1 0)	12.84	7.3	(0 4 0)	13.24	4.5
	(2 1 1)	17.08	14.1	(1 0 1)	14.39	13.2	(1 1 0)	15.51	23.3
	(1 2 0)	20.04	5.4	(2 1 0)	14.93	14.8	(0 0 1)	16.32	2.5
	(0 0 2)	20.55	8.5	(2 0 1)	16.31	32.6	(0 2 1)	17.55	25.0
	(2 2 0)	21.46	14.1	(4 0 0)	17.77	53.9	(1 3 0)	18.13	31.1
	(4 0 1)	22.07	29.6	(3 1 0)	18.32	9.6	(0 3 1)	19.02	5.6
	(1 2 1)	22.29	100.0	(0 1 1)	18.79	37.7	(0 6 0)	19.90	21.3
	(2 1 2)	24.60	14.7	(1 1 1)	19.04	13.9	(1 4 0)	20.38	4.6
	(5 1 1)	28.13	3.4	(3 0 1)	19.15	16.3	(0 4 1)	21.03	20.0
	(4 0 2)	28.50	5.1	(2 1 1)	20.38	83.9	(1 5 0)	22.32	12.5
	(1 2 2)	28.72	5.4	(4 1 0)	21.54	15.1	(1 0 1)	22.55	20.9
	(6 0 0)	29.04	4.8	(4 0 1)	22.54	88.2	(1 1 1)	23.28	100.0
	(1 3 0)	29.36	4.1	(1 2 0)	25.43	52.3	(1 2 1)	23.92	6.4
	(2 2 2)	30.02	3.9	(5 1 0)	25.60	42.7	(1 3 1)	24.48	5.6
	(2 3 0)	30.58	4.7	(4 1 1)	25.89	22.0	(0 6 1)	25.62	4.0
	(0 0 3)	31.11	16.9	(6 0 0)	26.80	100.0	(1 4 1)	26.44	7.8
	(1 0 3)	31.68	10.2	(3 2 0)	28.35	32.6	(1 5 1)	28.35	6.7
	(4 2 2)	34.60	2.8	(2 0 2)	28.97	43.6	(2 0 0)	29.12	11.5
	(4 3 1)	36.43	4.0	(6 1 0)	29.43	24.9	(1 6 1)	30.10	5.6
	(0 2 3)	36.72	4.5	(0 1 2)	30.25	47.2	(2 1 0)	30.63	7.2
	(2 3 2)	37.22	3.4	(4 2 0)	30.60	32.4	(2 2 0)	31.39	10.7
				(3 0 2)	31.06	7.4	(2 3 0)	31.92	5.6
				(6 1 1)	32.65	8.7	(2 4 0)	32.48	4.5
				(4 0 2)	33.16	18.0	(0 2 2)	33.52	3.7
				(4 2 1)	33.73	5.7	(0 3 2)	34.37	5.2
				(4 1 2)	34.32	14.4	(2 5 0)	35.05	4.3
				(5 0 2)	36.04	18.8	(0 4 2)	35.57	5.6
				(5 1 2)	37.90	9.0	(2 6 0)	36.53	3.5
				(6 0 2)	39.26	7.3	(0 5 2)	37.03	3.5
							(1 1 2)	37.47	4.9
							(1 2 2)	37.83	4.2
							(0 6 2)	38.86	4.2

the observed XRPD peaks, as well as the Miller indices assigned to these peaks and deduced from the indexing results.

It may be noted in passing that the unit cell parameters obtained for *S*-PG-Cl agreed very well with those obtained from a single-crystal study, and which have been published in the Cambridge Structural Database. [25] The existence of a different set of unit cell parameters for the (*S*-PG)–(*R*-PG-Cl) product that is different from the unit cell parameters of either of its coformers is proof that this isolated substance is an authentic salt–cocrystal.

On the other hand, the XRPD pattern of the (*S*-PG) + (*S*-PG-Cl) product could not be indexed to a single set of unit cell parameters. In fact, the XRPD pattern obtained by the simple numerical averaging of the XRPD patterns of *S*-PG and *S*-PG-Cl yielded a theoretical XRPD pattern that was the same as that of the (*S*-PG) + (*S*-PG-Cl) product. Collectively, these findings demonstrate the existence of stereoselectivity in the 2-phenylglycinol salt–cocrystal system, since no salt–cocrystal product was formed when *S*-PG and *S*-PG-Cl were subjected to the same solvent-assisted, solid-state grinding process as were *S*-PG and *R*-PG-Cl (which did yield a single crystalline phase).

The DSC thermograms obtained for the solid products are shown in Figure 3, and except for the *S*-PG-Cl product, these consisted of endothermic transitions that took place at relatively low temperatures. However, when the samples were heated isothermally at 110 °C for 15 min, the samples all lost less than approximately 0.25% of their total mass, demonstrating that these materials were obtain in the form of non-solvates.

The DSC melting endothermic transition of *S*-PG was observed to exhibit a temperature maximum at 78.2 °C (enthalpy of fusion equal to 160 J/g), while *S*-PG-Cl melted with decomposition at a temperature at 171 °C (enthalpy of fusion approximately equal to 120 J/g). The (*S*-PG) + (*S*-PG-Cl) product melted at a temperature (75.4 °C) that was nearly equal to that of *S*-PG, and the enthalpy associated with this transition (62.9 J/g) was approximately half that of *S*-PG. On the other hand, even though the (*S*-PG)–(*R*-PG-Cl) salt–cocrystal melted at the even lower temperature of 64.0 °C, the melting endotherm was characterized by a substantial (107 J/g) enthalpy of fusion.

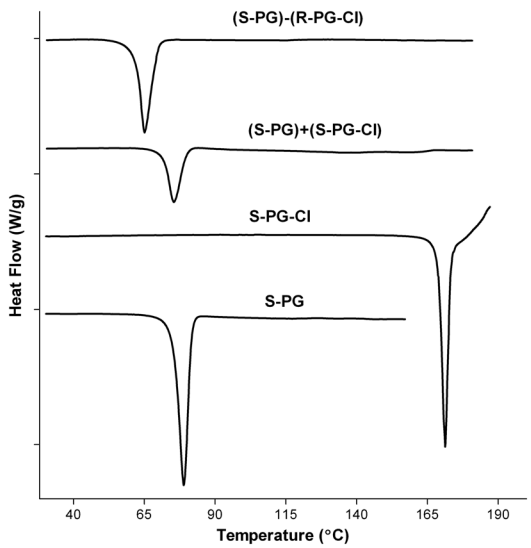

Fig. 3. Differential scanning calorimetry thermograms of (*S*)-phenylglycinol, (*S*)-phenyl-glycinol hydrochloride, the isolated yield of 1:1 (*S*)-phenylglycinol and (*S*)-phenyl-glycinol hydrochloride, and the 1:1 salt–cocrystal of (*S*)-phenylglycinol and (*R*)-phenylglycinol hydrochloride.

The Phenylglycine System

Because amino acids ordinarily exist in the solid state in their zwitterionic form, the amine and carboxylic acid groups are hydrogen bonded to each other and the carboxylate proton is partially transferred. However, this transfer is broken when a salt of the amino acid is formed, as has been demonstrated in the case of phenylalanine and phenylalanine hydrochloride. [26,27] Owing to the existence of both acidic and basic groups, phenylglycine is capable of forming salts with either basic or acidic reagents as long as the energy released upon proton transfer is larger than the energy required to break the hydrogen bonding of the zwitterion. Thus, the possibility of stereoselective salt–cocrystal formation in the phenylglycine system was investigated for both acidic and basic coformers.

Simple Phenylglycine Salts

The XRPD patterns of (*S*)-phenylglycine (i.e., *S*-PGLY), (*S*)-sodium phenylglycinate (i.e., *S*-Na-PGLY), and (*S*)-phenylglycine hydrochloride (i.e., *S*-PGLY-Cl) are shown in Figure 4. Although the diffraction patterns of *S*-PGLY and *S*-Na-PGLY are qualitatively similar, there are a sufficient number of differences between the two to demonstrate formation of the sodium salt. The three diffraction patterns were able to be indexed, and the derived unit cell parameters are found in Table 2. Also included in Table 2 are the scattering angles and relative intensities of the observed XRPD peaks, as well as the Miller indices assigned to these peaks and deduced from the indexing results. Only the single-crystal structure of the hydrochloride salt has been reported, [25] but the unit cell parameters reported in this article do not agree with those of the present study. This difference in unit cell parameters signifies that a different polymorphic form of *S*-PGLY-Cl has been obtained, which undoubtedly results from the methanol processing step used in the present work.

DSC was used to establish the properties of phenylglycine and its two salt forms, and the various thermograms are collected in Figure 5. The DSC thermograms of *S*-PGLY itself consisted of a single melting endothermic transition, which was characterized by a temperature maximum at 301 °C and an enthalpy of fusion equal to 298 J/g. The thermogram of

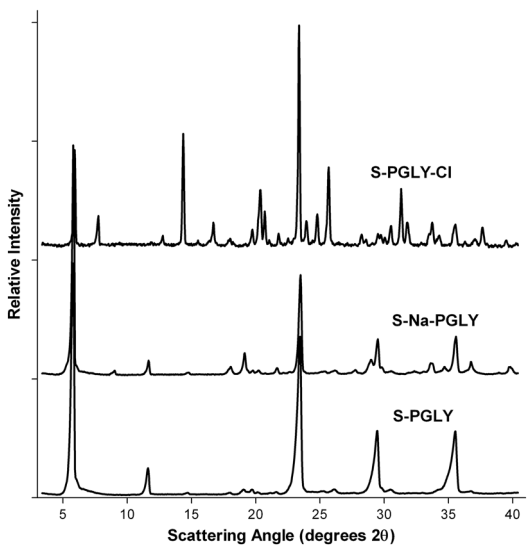

Fig. 4. X-ray powder diffraction patterns of (*S*)-phenylglycine, (*S*)-sodium phenylglycinate, and (*S*)-phenylglycine hydrochloride.

TABLE 2. Unit cell parameters obtained through indexing the X-ray diffraction patterns of (*S*)-phenylglycine, (*S*)-sodium phenylglycinate, and (*S*)-phenylglycine hydrochloride, and the indexed listing of scattering peaks

Unit cell parameter	(*S*)-Phenylglycine			(*S*)-Sodium phenylglycinate			(*S*)-Phenylglycine hydrochloride		
System	Monoclinic			Monoclinic			Monoclinic		
a	15.335 Å			15.342 Å			17.025 Å		
b	9.434 Å			9.826 Å			30.756 Å		
c	6.075 Å			5.369 Å			8.918 Å		
α	90°			90°			90°		
β	97.47°			98.12°			95.46°		
γ	90°			90°			90°		
	Miller index	Angle (degree 2)	Relative intensity	Miller index	Angle (degree 2)	Relative intensity	Miller index	Angle (degree 2)	Relative intensity
	(1 0 0)	5.77	100.0	(1 0 0)	5.80	100.0	(1 1 0)	5.91	47.6
	(2 0 0)	11.62	12.4	(0 1 0)	9.00	3.6	(1 2 0)	7.74	18.8
	(0 0 1)	14.66	2.1	(2 0 0)	11.65	7.8	(1 4 0)	12.75	10.4
	(3 0 0)	17.98	2.2	(2 1 0)	14.72	2.6	(0 5 0)	14.35	53.3
	(1 1 1)	19.04	3.5	(0 2 0)	18.04	5.2	(2 4 0)	15.51	8.5
	(1 2 0)	19.73	3.6	(0 1 1)	19.13	11.1	(3 2 0)	16.69	15.9
	(2 0 1)	20.17	2.4	(3 1 0)	19.77	3.6	(2 5 0)	17.85	8.8
	(2 1 1)	21.14	2.1	(1 1 1)	20.20	3.6	(1 6 0)	18.02	8.6
	(2 2 0)	21.60	2.5	(2 2 0)	21.68	4.6	(1 5 1)	18.23	7.9
	(4 0 0)	23.43	68.3	(2 0 1)	22.67	3.0	(3 1 1)	19.74	13.3
	(1 2 1)	25.18	2.8	(2 1 1)	23.47	43.9	(3 2 1)	20.37	29.5
	(3 1 1)	26.13	3.6	(3 2 0)	25.43	3.3	(0 2 2)	20.70	20.6
	(5 0 0)	29.45	28.3	(3 0 1)	26.18	3.7	(4 0 0)	21.03	8.6
	(2 3 0)	30.48	3.6	(1 3 0)	27.75	3.8	(4 2 0)	21.79	11.3
	(6 0 0)	35.53	28.1	(2 2 1)	28.97	8.2	(3 4 1)	22.49	9.0
	(6 1 1)	36.74	2.8	(2 3 0)	29.49	16.7	(2 0 2)	23.36	100.0
				(4 2 0)	29.79	5.0	(4 4 0)	23.93	16.8
				(4 0 1)	30.54	3.3	(4 2 1)	24.76	19.2
				(4 1 1)	32.33	3.2	(1 5 2)	25.66	39.9
				(1 3 1)	33.11	3.1	(4 5 1)	28.23	10.8
				(0 0 2)	33.67	6.6	(5 4 0)	28.58	9.1
				(5 2 0)	34.66	5.1	(5 2 1)	29.50	11.0
				(6 0 0)	35.58	17.8	(4 6 1)	29.73	11.3
				(6 1 0)	36.76	7.1	(5 5 0)	30.01	9.7
				(2 1 2)	38.93	2.8	(4 0 2)	30.51	14.8
				(1 2 2)	39.81	5.1	(5 4 1)	31.32	30.0
							(6 1 0)	31.78	16.0
							(6 3 0)	32.85	7.6
							(2 2 3)	33.51	11.2
							(6 4 0)	33.72	15.9
							(6 1 1)	34.26	10.8
							(3 0 3)	35.54	15.1
							(6 6 0)	36.28	7.8
							(6 5 1)	37.02	8.2
							(3 4 3)	37.63	14.1
							(6 1 2)	39.50	9.0

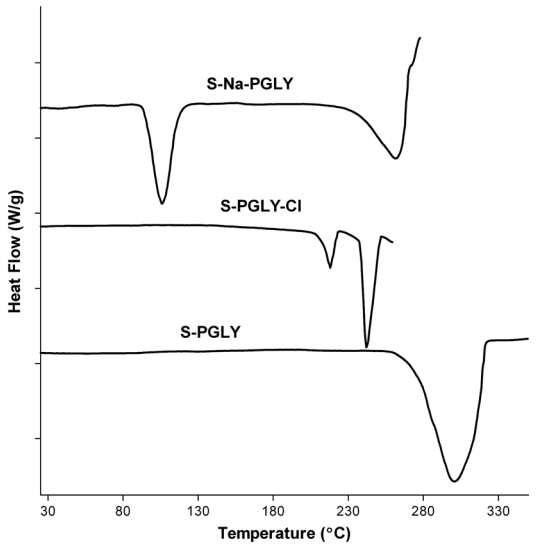

Fig. 5. Differential scanning calorimetry thermograms of (*S*)-phenylglycine, (*S*)-sodium phenylglycinate, and (*S*)-phenylglycine hydrochloride.

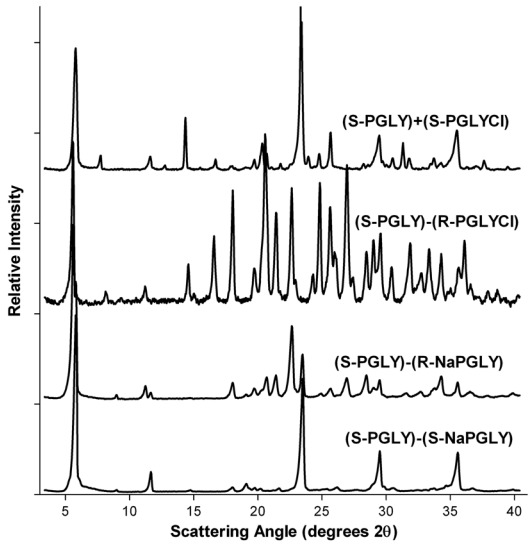

Fig. 6. X-ray powder diffraction patterns (XRPD) of the 1:1 salt–cocrystals of (*S*)-phenylglycine and (*S*)-sodium phenylglycinate, (*S*)-phenylglycine and (*R*)-sodium phenylglycinate, and (*S*)-phenylglycine and (*R*)-phenylglycine hydrochloride. Also shown is the XRPD pattern of the yield isolated after the attempted interaction of (*S*)-phenylglycine with (*S*)-phenylglycine hydrochloride.

the *S*-PGLY-Cl salt did not contain a desolvation endotherm but did exhibited two melting endotherms, indicating that the isolated product was the metastable polymorphic form. The first transition was characterized by a temperature maximum of 216 °C (enthalpy of fusion equal to 67 J/g), and the second transition was characterized by a temperature maximum of 242 °C (enthalpy of fusion equal to 246 J/g). The DSC thermograms of *S*-PGLY and *S*-PGLY-Cl were completely free of low-temperature endothermic transitions, demonstrating that these products were non-solvated.

The DSC thermogram of *S*-Na-PGLY contained a desolvation endotherm having a temperature maximum of 105 °C, associated with an enthalpy of desolvation equal to 209 J/g. The TVC of this product was determined to be 15.85%, which agrees well with the theoretically calculated weight loss that would be associated with a mono-methanol solvatomorph (i.e., 15.62%). The desolvated *S*-Na-PGLY product was subsequently observed to melt with decomposition at a temperature of 263 °C (because of the exothermic decomposition, the enthalpy of fusion could not be approximated).

Phenylglycine Salt–Cocrystals

The XRPD patterns of the products obtained by the interaction of 1:1 stoichiometric amounts of *S*-PGLY with *S*-Na-PGLY, *S*-PGLY with *R*-Na-PGLY, *S*-PGL with *S*-PGLY-Cl, and *S*-PGLY with *R*-PGLY-Cl are shown in Figure 6. Comparison of the diffraction patterns with those of their respective coformer compounds indicated that while new cocrystalline solids were formed by the interaction of (*S*)-phenylglycine with either enantiomer of sodium phenylglycinate, only the interaction of (*S*)-phenylglycine with (*R*)-phenylglycine hydrochloride led to the formation of a salt–cocrystal product.

The XRPD pattern of the solid isolated upon solvent-drop grinding of (*S*)-phenylglycine with (*S*)-phenylglycine hydrochloride was found to be simply the sum of the XRPD patterns of the starting materials, and not that of a new salt–cocrystal.

The authenticity of the three salt–cocrystal products was established by indexing their respective XRPD patterns, and the results of this analysis are collected in Table 3. Also included in Table 3 are the scattering angles and relative intensities of the observed XRPD peaks, as well as the Miller indices assigned to these peaks and deduced from the indexing results. It was found that the unit cell parameters derived from this analysis could account for all major peaks in the diffraction patterns of the (*S*-PGLY)–(*S*-Na-PGLY), (*S*-PGLY)–(*R*-Na-PGLY), and (*S*-PGLY)–(*R*-PGLY-Cl). The existence of different unit cells for the salt–cocrystal products relative to those of the coformer substances is definitive proof that these materials are authentic salt–cocrystal substances.

It is to be noted that the diffraction pattern obtained from the solid isolated by the attempted cocrystallization of *S*-PGLY with *S*-PGLY-Cl could not be indexed, demonstrating that this product consisted of more than one crystalline phase.

Thermal analysis was used to further study the stereoselectivity in the phenylglycine/phenylglycine hydrochloride system and the lack of stereoselectivity in the phenylglycine/sodium phenylglycinate system. As shown in Figure 7, the DSC thermograms of the (*S*-PGLY)–(*S*-Na-PGLY) and (*S*-PGLY)–(*R*-Na-PGLY) salt–cocrystal products both featured a prominent desolvation endotherms having temperature maxima in the range of 103–105 °C and which were associated with enthalpies of desolvation in the range of 95–100 J/g. The desolvated (*S*-PGLY)–(*S*-Na-PGYL) salt–cocrystal was subsequently observed to melt (with decomposition) at a temperature of 252 °C, while the desolvated (*S*-PGLY)–(*R*-Na-PGLY) salt–cocrystal melted with decomposition at a temperature of 258 °C.

The DSC thermogram of the non-solvated (*S*-PGLY)–(*S*-PGLY-Cl) salt–cocrystal consisted of a single melting endothermic transition, which was characterized by a temperature maximum at 247 °C and an enthalpy of fusion equal to 344 J/g. The DSC thermogram of the solid isolated after the attempted cocrystallization of (*S*)-phenylglycine with (*S*)-phenylglycine hydrochloride was found to strongly mimic the DSC thermogram of *S*-PGLY-Cl, although the enthalpies associated with the two thermally induced transitions were different in magnitude.

TABLE 3. Unit cell parameters obtained through indexing the X-ray diffraction patterns of the 1:1 salt–cocrystals of (*S*)-phenylglycine and (*S*)-sodium phenylglycinate, (*S*)-phenylglycine and (*R*)-sodium phenylglycinate, and (*S*)-phenylglycine and (*R*)-phenylglycine hydrochloride, and the indexed listing of scattering peaks

Unit cell parameter	(*S*)-Phenylglycine/(*S*)-Sodium phenylglycinate salt–cocrystal			(*S*)-Phenylglycine/(*R*)-sodium phenylglycinate salt–cocrystal			(*S*)-Phenylglycine/(*R*)-Phenylglycine hydrochloride salt–cocrystal		
System	Monoclinic			Triclinic			Triclinic		
a	9.824 Å			15.811 Å			10.960 Å		
b	2.655 Å			16.334 Å			15.999 Å		
c	15.156 Å			4.713 Å			6.471 Å		
α	90°			94.36°			99.98°		
β	90.54°			97.56°			100.53°		
γ	90°			75.51°			93.90°		
	Miller index	Angle (degree 2)	Relative intensity	Miller index	Angle (degree 2)	Relative intensity	Miller index	Angle (degree 2)	Relative intensity
	(0 0 1)	5.80	100.0	(0 1 0)	5.61	100.0	(0 1 0)	5.59	99.5
	(1 0 0)	8.99	2.7	(1 0 0)	5.81	69.1	(1 0 0)	8.15	12.7
	(0 0 2)	11.66	12.7	(0 2 0)	8.98	5.2	(0 2 0)	11.23	15.8
	(1 0 2)	14.73	2.5	(1 2 0)	11.24	10.3	(1 2 0)	14.59	27.5
	(2 0 0)	18.02	4.1	(2 1 0)	11.64	6.3	(2 0 0)	16.59	43.3
	(2 0 1)	19.11	6.1	(2 3 0)	18.03	11.8	(2 1 0)	18.05	70.2
	(1 0 3)	19.76	3.9	(0 0 1)	19.08	5.4	(1 1 1)	19.72	26.6
	(2 0 2)	21.63	3.5	(0 1 1)	20.28	7.8	(0 2 1)	20.57	100.0
	(0 0 4)	23.49	64.2	(1 0 1)	20.68	14.8	(2 2 0)	21.43	57.2
	(2 0 3)	25.38	3.3	(1 4 0)	21.43	16.1	(0 4 0)	22.63	69.7
	(3 0 0)	26.18	4.1	(0 2 1)	22.65	43.4	(1 2 1)	22.94	19.0
	(3 0 1)	27.67	2.6	(2 0 1)	23.48	27.8	(0 3 1)	24.29	21.6
	(0 0 5)	29.51	24.1	(3 4 0)	24.93	6.1	(3 0 0)	24.84	74.0
	(2 0 4)	29.83	4.4	(4 3 0)	25.68	8.7	(2 1 1)	25.63	58.3
	(1 0 5)	30.53	3.6	(3 1 1)	26.93	14.7	(3 1 0)	25.99	34.9
	(3 0 3)	32.41	2.5	(5 1 0)	28.47	16.0	(1 3 1)	26.94	82.5
	(0 1 0)	33.72	3.6	(5 2 0)	28.97	9.2	(0 5 0)	28.45	35.5
	(2 0 5)	34.69	5.1	(3 5 0)	29.50	13.4	(0 4 1)	28.99	41.8
	(1 1 0)	35.59	23.3	(3 3 1)	30.57	4.2	(2 4 0)	29.56	46.0
	(1 0 6)	36.71	3.5	(4 1 1)	31.57	6.2	(1 5 0)	30.41	26.7
	(2 1 1)	38.94	2.3	(5 4 0)	32.69	6.9	(3 3 0)	31.88	40.4
	(1 1 3)	39.85	2.9	(4 3 1)	33.78	9.0	(0 2 2)	32.74	23.3
				(3 6 0)	34.29	15.4	(4 0 0)	33.35	36.8
				(5 5 0)	35.58	12.1	(0 5 1)	34.28	33.5
				(5 1 1)	36.55	7.0	(2 5 0)	34.82	13.9
				(5 3 1)	37.90	4.8	(3 2 1)	35.02	14.9
				(0 1 2)	39.04	4.7	(1 2 2)	35.60	26.7
				(2 6 1)	39.88	6.2	(2 0 2)	36.11	40.4
							(4 2 0)	36.58	16.8
							(2 1 2)	37.93	13.5
							(1 3 2)	38.69	14.4
							(4 1 1)	40.34	9.7

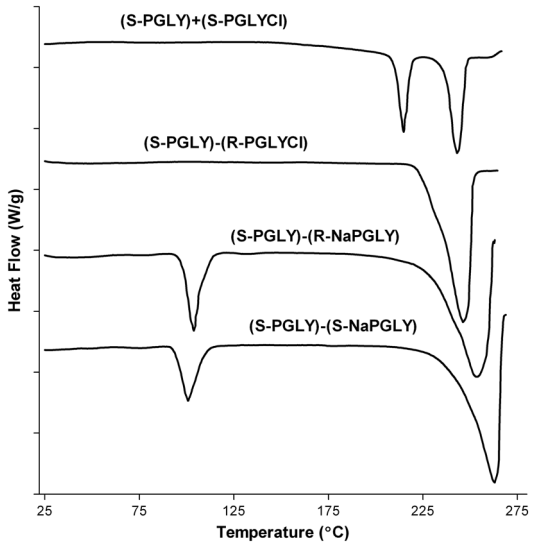

Fig. 7. Differential scanning calorimetry (DSC) thermograms of the 1:1 salt–cocrystals of (*S*)-phenylglycine and (*S*)-sodium phenylglycinate, (*S*)-phenylglycine and (*R*)-sodium phenylglycinate, and (*S*)-phenylglycine and (*R*)-phenylglycine hydrochloride. Also shown is the DSC thermogram pattern of the yield isolated after the attempted interaction of (*S*)-phenylglycine with (*S*)-phenylglycine hydrochloride.

The TVCs measured for both the (*S*-PGLY)–(*S*-Na-PGLY) and (*S*-PGLY)–(*R*-Na-PGLY) salt–cocrystal products were both approximately 4.75%, which agrees reasonably well with the theoretically calculated weight loss that would be associated with a hemi-methanol solvatomorph (i.e., 4.57%). This finding is reasonable, considering that the sodium phenylglycinate coformer was a mono-methanol solvatomorph, and the phenylglycine coformer is non-solvated.

CONCLUSIONS

The accumulating body of work has demonstrated that the phenomenon of salt–cocrystal formation appears to be quite general, and that such products can be readily formed by the interaction of appropriate coformer reactants. However, when the cocrystal formers contain centers of dissymmetry, it has been learned that formation of the salt–cocrystal product can be complicated by stereoselective effects.

In the systems studied thus far, it has been found that cocrystallization of an enantiomerically pure basic or zwitterionic substance (i.e., α-methylbenzylamine, 2-phenylglycinol, or 2-phenylglycine) with its enantiomerically pure acid addition salt (i.e., its hydrochloride salt) only takes place when the absolute configuration of the two reactants is opposite. No cocrystal formation has been detected for a base and its hydrochloride salt when both coformers are of the same absolute configuration. This finding indicates that such coformers of the same configuration cannot pack efficiently, and instead crystallize separately.

On the other hand, no stereoselectivity has been detected in the one system studied that entailed cocrystallization of an enantiomerically pure acidic or zwitterionic substance (i.e., 2-phenylglycine) with its enantiomerically pure base addition salt (i.e., its sodium salt). More work is currently being conducted with related systems to learn if the carboxylate–cation interaction is sufficiently strong so as to override crystal packing effects that clearly exist with amino–anion interactions.

LITERATURE CITED

1. Vishweshwar P, McMahon JA, Bis JA, Zaworotko MJ. Pharmaceutical cocrystals. J Pharm Sci 2006;95:499–516.
2. Shan N, Zaworotko MJ. The role of cocrystals in pharmaceutical science. Drug Discov Today 2008;13:440–446.
3. Frišči T, Jones W. Benefits of cocrystallization in pharmaceutical materials science: an update. J Pharm Pharmacol 2010;62:1547–1559.
4. Good DJ, Rodríguez-Hornedo N. Solubility advantage of pharmaceutical cocrystals, Cryst Growth Design 2009;9:2252–2264.
5. Bethune SJ, Huang N, Jayasanka A, Rodríguez-Hornedo N. Understanding and predicting the effect of cocrystal components and pH on cocrystal solubility. Cryst Growth Design 2009;9:3976–3988.
6. Aakeröy CB, Forbes S, Desper J. Using cocrystals to systematically modulate aqueous solubility and melting behavior of an anticancer drug. J Am Chem Soc 2009;131:17048–17049.
7. Aakeröy C, Salmon DJ. Building co-crystals with molecular sense and supramolecular sensibility. CrystEngComm 2005;7:439–448.
8. Schultheiss N, Newman A. Pharmaceutical cocrystals and their physicochemical properties. Cryst Growth Design 2009;9:2950–2967.
9. Aakeröy C, Fasulo ME, Desper J. Cocrystal or salt: does it really matter? Mol Pharm 2007;4:317–322.
10. Childs SL, Stahly GP, Park A. The salt-cocrystal continuum: the influence of crystal structure on ionization state. Mol Pharm 2007;4:323–338.
11. Aakeröy CB, Rajbanshi A, Li ZJ, Desper J. Mapping out the synthetic landscape for recrystallization, cocrystallization, and salt formation. CrystEngComm 2010;12:4231–4239.
12. Schultheiss N, Lorimer K, Wolfe S, Desper J. Attempted construction of minoxidil: carboxylic acid cocrystals; 7 salts and 1 cocrystal resulted. CrystEngComm 2010;12:742–749.
13. Brittain HG. Vibrational spectroscopic studies of cocrystals and salts. 2. The benzylamine-benzoic acid system. Cryst Growth Design 2009;9:3497–3503.
14. Brittain HG. Vibrational spectroscopic studies of cocrystals and salts. 3. Cocrystal products formed by benzenecarboxylic acids and their sodium salts. Cryst Growth Design 2010;10:1990–2003.
15. Chen S, Xi H, Henry RF, Marsden I, Zhang GGZ. Chiral cocrystal solid solution: structures, melting point phase diagram, and chiral enrichment of (ibuprofen)$_2$(4,4-dipyridyl) CrystEngComm 2010;12:1485–1493.
16. Brittain HG. Vibrational spectroscopic studies of cocrystals and salts. 4. Cocrystal products formed by benzylamine, α-methylbenzylamine, and their chloride salts. Cryst Growth Design 2011;11:2500–2509.
17. Gould PL. Salt selection for basic drugs. Int J Pharm 1986;33:201–217.
18. Metrangolo P, Pilati T, Terraneo G, Biella S, Resnati G. Anion coordination and anion-templated assembly under halogen bonding control. CrystEngComm 2009;11:1187–1196.
19. Childs SL, Chyall LJ, Dunlap JT, Smolenskaya VN, Stahly BC, Stahly GP. Crystal engineering approach to forming cocrystals of amine hydrochlorides with organic acids: molecular complexes of fluoxetine hydrochloride with benzoic, succinic, and fumaric acids. J Am Chem Soc 2004;126:13335–13342.
20. Pop M, Sieger P, Cains PW. Tiotropium fumarate: an interesting pharmaceutical cocrystal. J Pharm Sci 2009;98:1820–1834.
21. Boultif A, Louër D. Powder pattern indexing with the dichotomy method. J Appl Cryst 2004;37:724–731.
22. Visser JW. A fully automatic program for finding the unit cell from powder data. J Appl Cryst 1969;2:89–95.
23. Altomare A, Giacovazzo C, Guagliardi A, Moliterni AGG, Rizzi R, Werner P-E. New techniques for indexing: N-TREOR in EXPO. J Appl Cryst 2000;33:1180–1186.
24. Trask AV, Jones W. Crystal engineering of organic cocrystals by the solid-state grinding approach. Top Curr Chem 2005;254:41–70.
25. Bohme U, Wiesner S. Crystal structure file VECWUW. Cited as a private communication to the Cambridge Structural Database (2005).
26. Al-Jaraggiyku AR, Koetzle TF. Neutron diffraction study of L-phenylalanine hydrochloride. Acta Cryst 1975;B31:2461–2465.
27. Ravichandran S, Dattagupta JK, Chakrabarti C. D-phenylglycine hydrochloride. Acta Cryst 1998;C54:499–501.